Fundamental Physics via Gravitational-Wave Observation

Kipp CANNON for the LIGO Scientific Collaboration, Virgo Collaboration, and KAGRA Collaboration
LIGO-G2302137

Gravitational Wave Probes of Physics Beyond Standard Model,
Osaka Metropolitan University, 2023-11-07

Gravitational-Wave Astronomy

- What are gravitational waves?
- Sources of gravitational waves?
- No time to discuss this;
- I'm assuming you've heard these things already, I'm diving right in ...

LIGO-Virgo-KAGRA Observation Schedule

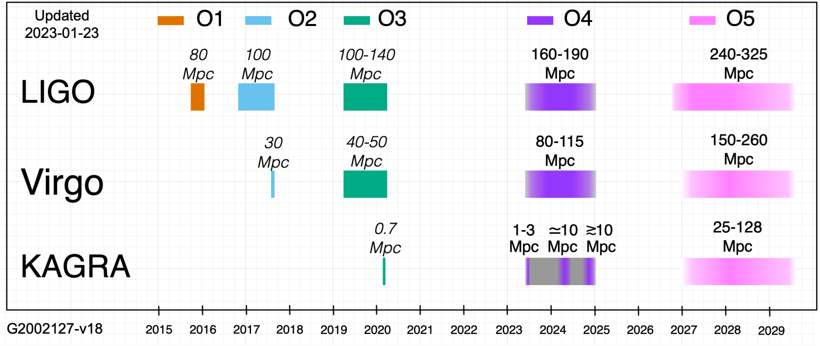

- See https://observing.docs.ligo.org/plan/

Speed of Gravity

- arXiv:1706.01812 [gr-qc]: "**GW170104: Observation of a 50-Solar-Mass Binary Black Hole Coalescence at Redshift 0.2**"

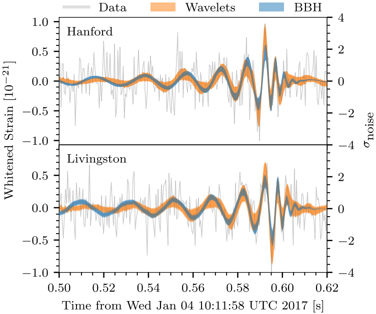

FIG. 4. Time-domain detector data (gray), and 90% confidence intervals for waveforms reconstructed from the morphology-independent wavelet analysis (orange) and binary black hole (BBH) models from both waveform families (blue), whitened by each instrument's noise amplitude spectral density. The left ordinate axes are normalized such that the amplitude of the whitened data and the physical strain are equal at 200 Hz. The right ordinate axes are in units of noise standard deviations. The width of the BBH region is dominated by the uncertainty in the astrophysical parameters.

- The fact that the signal still looks liked a compact object after such a long distance bounds the amount of dispersion and thus the mass of graviton to $m_g \leq 7.7 \times 10^{-23}\ \mathrm{eV/c^2}$

Speed of Gravity

- arXiv:1811.00364 [gr-qc]: "**Tests of General Relativity with GW170817**"
- Figures 1 & 2.

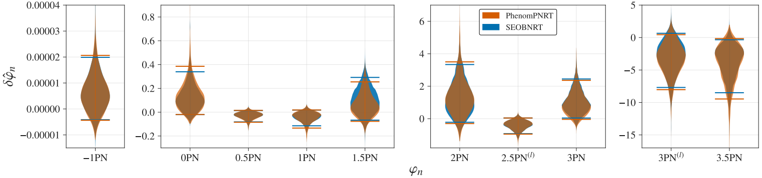

FIG. 1. Posterior density functions on deviations of PN coefficients $\delta\hat{\varphi}_n$ obtained using two different waveform models (`PhenomPNRT` and `SEOBNRT`); see the main text for details. The −1PN and 0.5PN corrections correspond to absolute deviations, whereas all others represent fractional deviations from the PN coefficient in GR. The horizontal bars indicate 90% credible regions.

- constraints on departures from GR using parametric waveform models similar to observed with black holes, but because of the long inspiral this was the first relatively strict measurement of the dipole radiation component. still 2 orders of magnitude weaker than constraint inferred from PSR J0737-3039.
- dispersion bounds mass of graviton to be $m_g \leq 9.51 \times 10^{-22}\,\mathrm{eV/c^2}$

Speed of Gravity

- arXiv:1710.05834 [astro-ph.HE]: “**Gravitational Waves and Gamma-Rays from a Binary Neutron Star Merger: GW170817 and GRB 170817A**”

- Figure 2.

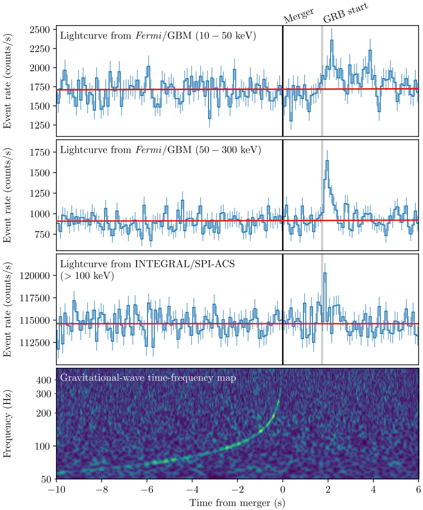

Figure 2. Joint, multi-messenger detection of GW170817 and GRB 170817A. Top: the summed GBM lightcurve for sodium iodide (NaI) detectors 1, 2, and 5 for GRB 170817A between 10 and 50 keV, matching the 100 ms time bins of the SPI-ACS data. The background estimate from Goldstein et al. (2016) is overlaid in red. Second: the same as the top panel but in the 50–300 keV energy range. Third: the SPI-ACS lightcurve with the energy range starting approximately at 100 keV and with a high energy limit of least 80 MeV. Bottom: the time-frequency map of GW170817 was obtained by coherently combining LIGO-Hanford and LIGO-Livingston data. All times here are referenced to the GW170817 trigger time T_0^{GW}.

Speed of Gravity

- Assuming up to tens of seconds of difference in emission time,

$$-3 \times 10^{-15} \leq \frac{\Delta v}{v_{\mathrm{EM}}} \leq +7 \times 10^{-16}.$$

- With knowledge of the gravitational potentials through which the waves travelled, the time delay provides a constraint on the difference in how much gravity and EM violate the equivalence principle. Combined with existing constraints on EM's (non)violation of the equivalence principle, this becomes a constraint on GW's violation of the EP.
- Using only the galaxy's potential, the difference in fractional deviations in the Shapiro delay is

$$-2.6 \times 10^{-7} \leq \gamma_{\mathrm{GW}} - \gamma_{\mathrm{EM}} \leq 1.2 \times 10^{-6}.$$

Expansion History of the Universe

- Hubble parameter and dark energy constraints
- GWs from a compact object merger have precisely predicted intrinsic amplitude given mass parameters: observed amplitude at Earth gives distance to source
- for BBHs red-shift is exactly degenerate with mass so the red-shift cannot be measured from the GWs alone
- if the source's host galaxy can be identified the EM red-shift can be used
- error box is too large to identify a unique galaxy, but an ensemble of host galaxies can be obtained, each having it's own probability of being the host, providing a distribution of red shifts, and therefore a (broad) posterior PDF for H_0
- with many many observations the joint posterior should eventually converge

Expansion History of the Universe

- arXiv:1901.01540 [astro-ph.CO]: "**First measurement of the Hubble constant from a dark standard siren using the Dark Energy Survey galaxies and the LIGO/Virgo binary–black–hole merger GW170814**"
- arXiv:1908.06060 [astro-ph.CO]: "**A gravitational-wave measurement of the Hubble constant following the second observing run of Advanced LIGO and Virgo**"

Expansion History of the Universe

- compare posterior from all BBHs in O1+O2 to posterior from GW170817 alone, for which a lone host galaxy was identified using an optical observation.

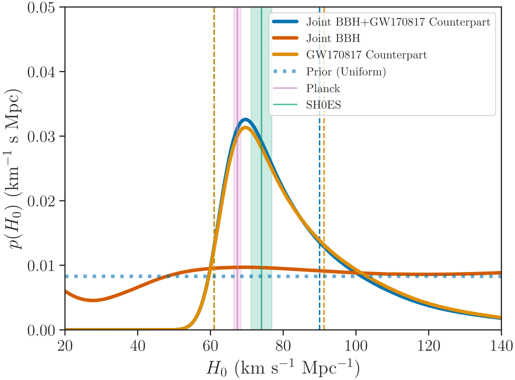

Expansion History of the Universe

- arXiv:2111.03604 [astro-ph.CO]: "**Constraints on the cosmic expansion history from GWTC–3**"
- Adding all O3 BBHs tightens the constraint slightly

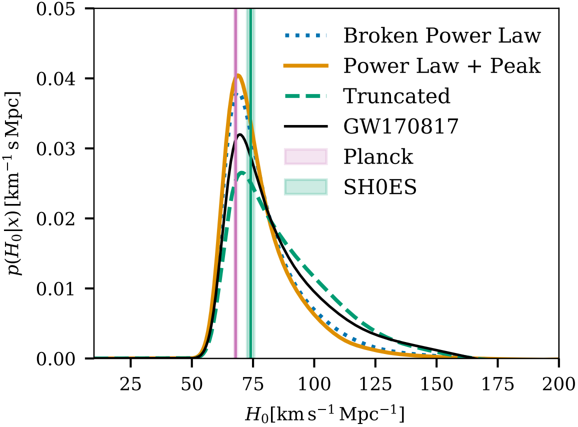

Sub-solar Mass Compact Objects

- dark matter, primordial black holes
- Not a new activity. 2007 student PhD thesis described the design, operation, and results of a search for MACHOs:
  - arXiv:0705.1514 [gr-qc]: "**Searching for Gravitational Radiation From Binary Black Hole MACHOs in the Galactic Halo**"
- More recent results:
  - arXiv:1904.08976 [astro-ph.CO]: "**Search for sub-solar mass ultracompact binaries in Advanced LIGO's second observing run**"
  - arXiv:2109.12197 [astro-ph.CO]: "**Search for subsolar-mass binaries in the first half of Advanced LIGO and Virgo's third observing run**"
- Latest result:
  - arXiv:2212.01477 [astro-ph.HE]: "**Search for subsolar-mass black hole binaries in the second part of Advanced LIGO's and Advanced Virgo's third observing run**"

Sub-solar Mass Compact Objects

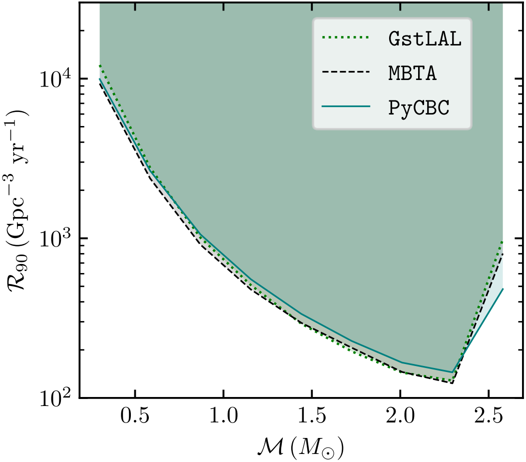

Figure 2. Merger rate limits as function of the source frame chirp mass of the binary system, in data from the full O3. The dotted, dashed and solid lines represent the 90% confidence limits obtained by `GstLAL`, `MBTA` and `PyCBC`, respectively.

Sub-solar Mass Compact Objects

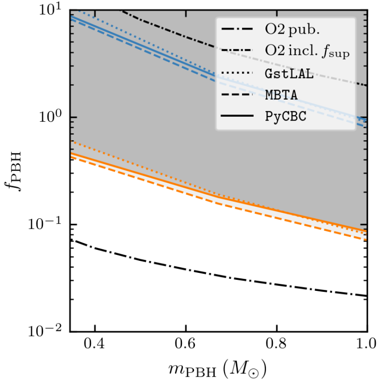

Figure 4. Constraints on DM fraction of PBHs, f_{PBH}, for a monochromatic mass function and assuming the merger rates for early PBH binaries from Hütsi et al. (2021) (orange) and late PBH binaries from Phukon et al. (2021) (blue). Shown in black are results for SSM searches in O2 (Abbott et al. 2019b) with and without the rate suppression factor f_{sup}. For the first time, $f_{\mathrm{PBH}} = 1$ for early binaries is excluded in the whole SSM range probed by this search.

Sub-solar Mass Compact Objects

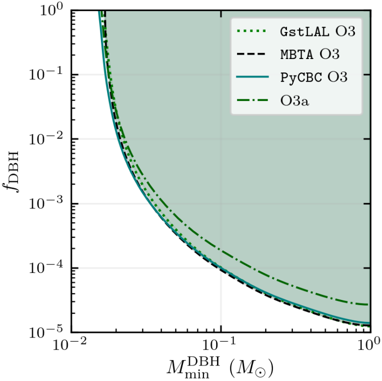

Figure 5. Constraints on the abundance of DBHs, $f_{\rm DBH}$, as a function of the lower limit of the DBH mass distribution, $M_{\rm min}^{\rm DBH}$ from O3 data for the 3 search pipelines: `GstLAL` (*dotted*), `MBTA` (*dashed*) and `PyCBC` (*solid*). Constraints from the search for SSM compact objects in O3a data (Abbott et al. 2022) are shown for comparison.

Axions

- GWs from axion clouds condensed around spinning black holes:
  - arXiv:1812.09622 [astro-ph.HE]: “**A first search for a stochastic gravitational-wave background from ultralight bosons**”
-

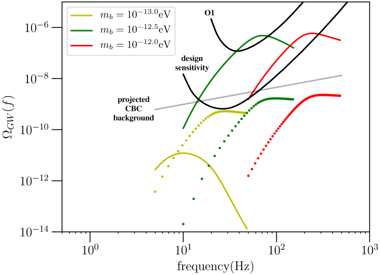

FIG. 2. Energy density spectra in the LIGO band overlapped with the power-law integrated curves [36] of LIGO O1 [65] and design sensitivity [66]. Solid curves are spectra based on the isolated BH model with uniform distribution of $\chi \in [0, 1.0]$, whereas dotted curves represent spectra with the BBH merger remnant model. The gray line indicates the projected background of compact binary coalescence (CBC) modeled as a simple power-law spectrum with a power law index of 2/3 [17]. The solid yellow curve is much lower than the other curves, because of the predicted lack of isolated BHs with large enough mass to couple to scalar fields with $m_b = 10^{-13}$ eV.

Axions

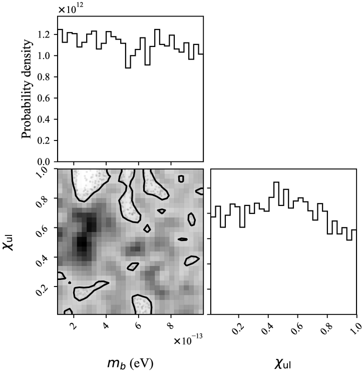

FIG. 7. Posterior results given by the data from the first Advanced LIGO observing run, recovered with the $\chi_{\rm ul}$ parameterization. The contour on the two-dimensional posterior represents the 95% confidence level.

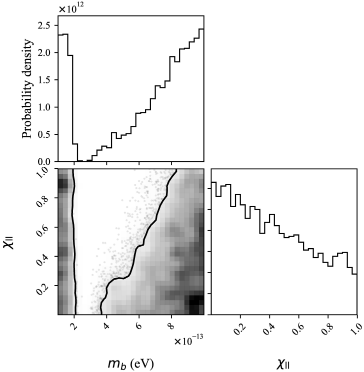

FIG. 8. Posterior results given by the data from the first Advanced LIGO observing run, recovered with the $\chi_{\rm ll}$ parameterization. The contour on the two-dimensional posterior represents the 95% confidence level.

Axions

- Same physics, but search targets nearby sources visible as isolated CW tones:
  - arXiv:2111.15507 [astro-ph.HE]: "**All-sky search for gravitational wave emission from scalar boson clouds around spinning black holes in LIGO O3 data**"
- Constraint depends on presence of a suitable nearby ($\lesssim 10\,\mathrm{kpc}$) spinning black hole, the existence of which we cannot confirm.
- If any such source exists, the excluded axion mass is essentially the same as obtained from the stochastic search.

Axions

- Amplification of GWs passing through an axion dark matter halo in axion-Chern-Simons gravity.
- In this theory GWs can stimulate axion decay into gravitons, producing a GW echo.
- Absence of a detected echo constraints the coupling constant.
- arXiv:2303.07688 [hep-ph]: “**Observational constraint on axion dark matter in a realistic halo profile with gravitational waves**”
- 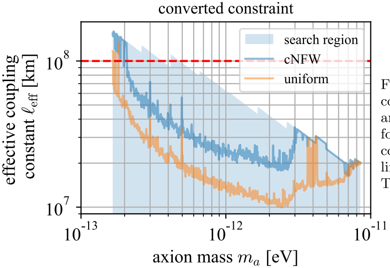

FIG. 7. The combined constraint on the effective coupling constant $\ell_{\rm eff}$ as a function of the axion mass m_a from the analysis of five GW events. The blue line is the constraints for the core NFW profile, while the orange one is the previous constraints [21] for the uniform DM profile. The red dashed line is the constraint from Gravity Probe B [22] for $f_{\rm DM} = 1$. The faint blue region is the searched parameter space.

Departures from GR

- Already mentioned tests of departures from GR using parametric waveform models above, in the context of the speed of gravity and constraints on the mass of the graviton (GW dispersion).
- O2: arXiv:2010.14529 [gr-qc]: "**Tests of General Relativity with Binary Black Holes from the second LIGO–Virgo Gravitational-Wave Transient Catalog**"
- O3: arXiv:2112.06861 [gr-qc]: "**Tests of General Relativity with GWTC-3**"

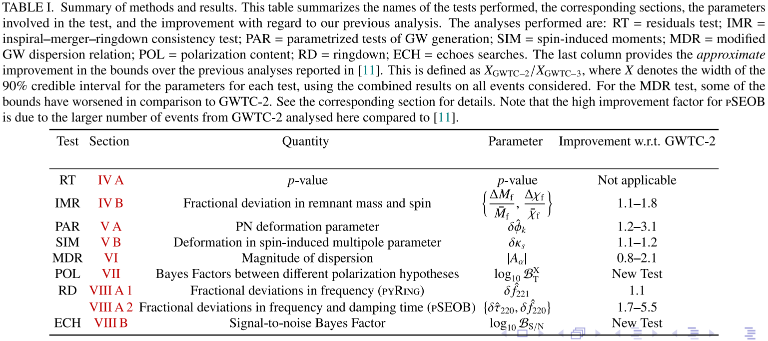

TABLE I. Summary of methods and results. This table summarizes the names of the tests performed, the corresponding sections, the parameters involved in the test, and the improvement with regard to our previous analysis. The analyses performed are: RT = residuals test; IMR = inspiral–merger–ringdown consistency test; PAR = parametrized tests of GW generation; SIM = spin-induced moments; MDR = modified GW dispersion relation; POL = polarization content; RD = ringdown; ECH = echoes searches. The last column provides the *approximate* improvement in the bounds over the previous analyses reported in [11]. This is defined as $X_{\mathrm{GWTC-2}}/X_{\mathrm{GWTC-3}}$, where X denotes the width of the 90% credible interval for the parameters for each test, using the combined results on all events considered. For the MDR test, some of the bounds have worsened in comparison to GWTC-2. See the corresponding section for details. Note that the high improvement factor for pSEOB is due to the larger number of events from GWTC-2 analysed here compared to [11].

Test	Section	Quantity	Parameter	Improvement w.r.t. GWTC-2
RT	IV A	p-value	p-value	Not applicable
IMR	IV B	Fractional deviation in remnant mass and spin	$\left\{\frac{\Delta M_{\mathrm{f}}}{\bar{M}_{\mathrm{f}}}, \frac{\Delta \chi_{\mathrm{f}}}{\bar{\chi}_{\mathrm{f}}}\right\}$	1.1–1.8
PAR	V A	PN deformation parameter	$\delta\hat{\phi}_k$	1.2–3.1
SIM	V B	Deformation in spin-induced multipole parameter	$\delta\kappa_s$	1.1–1.2
MDR	VI	Magnitude of dispersion	$\lvert A_\alpha \rvert$	0.8–2.1
POL	VII	Bayes Factors between different polarization hypotheses	$\log_{10} \mathcal{B}_{\mathrm{T}}^{\mathrm{X}}$	New Test
RD	VIII A 1	Fractional deviations in frequency (pyRing)	$\delta\hat{f}_{221}$	1.1
	VIII A 2	Fractional deviations in frequency and damping time (pSEOB)	$\{\delta\hat{\tau}_{220}, \delta\hat{f}_{220}\}$	1.7–5.5
ECH	VIII B	Signal-to-noise Bayes Factor	$\log_{10} \mathcal{B}_{\mathrm{S/N}}$	New Test

Departures from GR

- IMR test: measure total mass and angular momentum during inspiral phase; predict mass and spin of final black hole using GR; measure mass and spin during ring-down phase and compare.

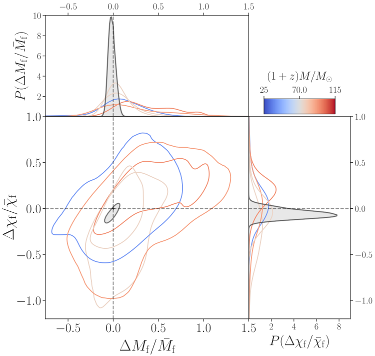

FIG. 3. Combined results of the IMR consistency test for BBH events which satisfy the selection criteria (see Table IV and Appendix B). The combined bounds are obtained assuming the same deviation for all events. The main panel shows the 90% credible regions of the 2D posteriors on $(\Delta M_f/\bar{M}_f, \Delta\chi_f/\bar{\chi}_f)$ assuming a uniform prior, with $(0,0)$ being the expected value for GR. The side panels show the marginalized posterior on $\Delta M_f/\bar{M}_f$ and $\Delta\chi_f/\bar{\chi}_f$. The gray distributions correspond to posteriors obtained by combining individual results. The other colored traces correspond to the O3b events given in Table IV where the color encodes the median redshifted total mass.

Non-GR Polarization States

- To directly observe N polarizations requires N (single polarization) antennas.
- GR says $N = 2$, we have 3 antennas, so we can test for a 3rd polarization component, but the two LIGO antennas sense nearly the same polarization so in practice there are no useful constraints on a 3rd DOF from direct observations of the strain field.
- Need a 4th detector — **KAGRA** — to directly test for $N \geq 2$ polarizations
- Indirect constraints come from observing the phase evolution of compact object mergers: more polarizations = higher rate of energy loss than predicted by GR.
- Already mentioned the test for dipole radiation from GW170817, above in the context of the speed of gravity test.

Non-GR Polarization States

- Another example, scalar modes:
  - arXiv:2105.00253 [gr-qc]: “**Scalar-tensor mixed polarization search of gravitational waves**”
  - scalar-to-tensor amplitude ratio constraint:

$$\begin{aligned} &\text{GW170814:} && R_{\mathrm{ST}} \leq 0.20 \\ &\text{GW170817:} && R_{\mathrm{ST}} \leq 0.0068 \end{aligned}$$

- Searches for non-GR polarizations (in non-existent signals):
  - arXiv:1709.09203 [gr-qc]: “**First search for nontensorial gravitational waves from known pulsars**”
  - arXiv:1802.10194 [gr-qc]: “**A Search for Tensor, Vector, and Scalar Polarizations in the Stochastic Gravitational-Wave Background**”

Birefringence

- Polarization-dependant wave propagation.
- Check for difference in speed for left- and right-hand circularly polarized GWs:
  - arXiv:2109.09718 [astro-ph.HE]: "**Tests of Gravitational-Wave Birefringence with the Open Gravitational-Wave Catalog**"
  - Constraint is on M_{PV}^{-1} which has units of energy, and described as "energy scale at which higher order modification starts to be relevant", but the exact meaning is unclear because they also use it to absorb the values of two unknown dimensionless constants.
  - GR corresponds to $M_{\mathrm{PV}}^{-1} = 0\,\mathrm{eV}^{-1}$.
  - If their statistics are correct, 2 of 94 signals analyzed showed $\sim 3\sigma$ excursions from GR, which is too many for random chance.
  - GW190521 & GW191109.

Birefringence

- Test for mixing of GR tensor GW modes with scalar or vector degrees of freedom.
- In (non-GR) Lorentz-invariant theories vacuum FRW spacetime does not allow mixing to occur, but presence of inhomogeneities can induce mixing.
- Isolate the two polarization components of a merger waveform, and test for an arrival time difference.
- arXiv:2301.04826 [gr-qc]: "**Probing lens-induced gravitational-wave birefringence as a test of general relativity**"

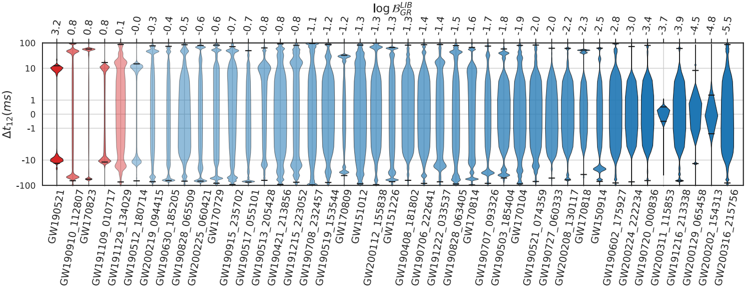

Large Extra Dimensions

- GW170817's luminosity distance / red-shift distance agreement as a constraint on large extra dimensions
- arXiv:1801.08160 [gr-qc]: "**Limits on the number of spacetime dimensions from GW170817**"

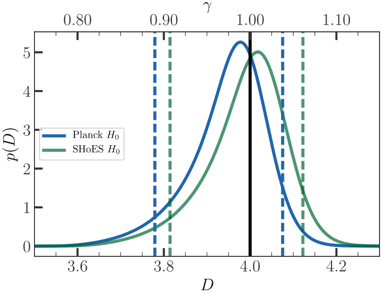

Figure 1. Posterior probability distribution for the number of spacetime dimensions, D, using the GW distance posterior to GW170817 and the measured Hubble velocity to its host galaxy, NGC 4993, assuming the H_0 measurements from Planck Collaboration et al. (2016) (blue curve) and Riess et al. (2016) (green curve). The dashed lines show the symmetric 90% credible intervals. The equivalent constraints on the damping factor, γ, are shown on the top axis. GW170817 constrains D to be very close to the GR value of $D = 4$ spacetime dimensions, denoted by the solid black line.

- Implications for LISA
  - arXiv:2109.08748 [gr-qc]: "**Constraining cosmological extra dimensions with gravitational wave standard sirens: from theory to current and future multi-messenger observations**"

Nuclear Physics

- Testing for transition to unconstrained quarks in NS interiors:
  - arXiv:2310.13603 [astro-ph.HE]: "**On the Testability of the Quark-Hadron Transition Using Gravitational Waves From Merging Binary Neutron Stars**"
- GW170817: prompt collapse to BH or not, implications for EOS:
  - arXiv:1710.05834 [astro-ph.HE]: "**Gravitational Waves and Gamma-Rays from a Binary Neutron Star Merger: GW170817 and GRB 170817A**"
  - arXiv:1805.11579 [gr-qc]: "**Properties of the binary neutron star merger GW170817**"
- Pair production instability supernova bound:
  - arXiv:2009.01075 [gr-qc]: "**GW190521: A Binary Black Hole Merger with a Total Mass of** $150\,\mathrm{M}_\odot$"

Strings

- Cosmic strings.
- Dynamics of perturbations on strings lead to GW emission.
- Depending on nature of string network, GW flux might be a stochastic background or a population of distinct transient signals.
- Search for predicted signals using normal transient search techniques and/or stochastic search techniques.
- arXiv:2101.12248 [gr-qc]: "**Constraints on cosmic strings using data from the third Advanced LIGO–Virgo observing run**"
- For non-GW reasons I don't understand, it is argued that string networks that would tend to produce impulsive burst events instead of a stochastic background are disfavoured, therefore in the parameter space covered in the latest searches the stochastic results provide the tightest bounds.

Dark Photon

- arXiv:2105.13085 [gr-qc]: "**Constraints on dark photon dark matter using data from LIGO's and Virgo's third observing run**"
- Based on possibility that dark matter interacts directly with the GW interferometer.
  - Assumes dark photon has some mass, and vector potential couples to a baryon or (baryon − lepton) current via a term in the Lagrangian.

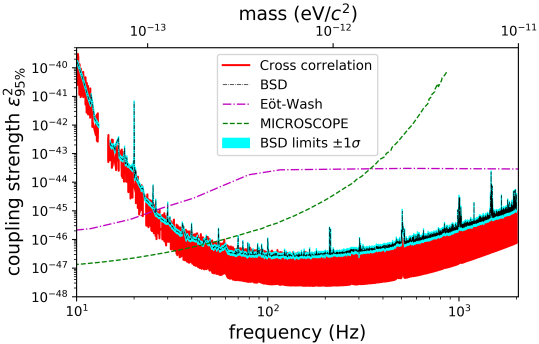

Summary

So you want to constrain your model? Past successful constraints computed

- The effect it would have on compact object merger waveforms:
  - at the source,
  - or in transit.
- The effect it would have on compact object mergers:
  - number density vs distance,
  - mass,
  - spin,
  - spin alignment,
  - ...
- The effect it would have on the interferometer itself:
  - interactions with the test masses,
  - long-distance correlations.

Pro Tips

Likely to require going back to the drawing board:

- stochastic spectra that are quieter than other, expected, stochastic sources,
- modifications of compact object merger waveforms that are exactly or nearly degenerate with conventional source parameters,

If you try yourself, be careful not to:

- assume the noise is Gaussian,
  - OK for a null result, but claiming a discovery of a new phenomenon will requier a better understanding of the noise than this.
  - You will need a technique for constructing a signal-free data surrogate.
- construct an *a posteriori* detection statistic.
  - Very serious. No matter how honest you believe yourself to be, you are not as honest as you believe and this is never ever OK.